

RJUA-MedDQA: A Multimodal Benchmark for Medical Document Question Answering and Clinical Reasoning

Congyun Jin*
 Yujiao Li
 Yingbo Wang
 Yabo Jia
 Ant Group
 Shanghai, China

Ming Zhang*
 Weixiao Ma
 Chenfei Chi
 Xiangguo Lv
 Renji Hospital
 Shanghai, China §

Fangzhou Li
 Wei Xue
 Yiran Huang†
 Renji Hospital
 Shanghai, China §

Tao Sun
 Haowen Wang
 Yuliang Du
 Cong Fan‡
 Jinjie Gu
 Ant Group
 Shanghai, China

ABSTRACT

Recent advancements in Large Language Models (LLMs) and Large Multi-modal Models (LMMs) have shown potential in various medical applications, such as Intelligent Medical Diagnosis. Although impressive results have been achieved, we find that existing benchmarks do not reflect the complexity of real medical reports and specialized in-depth reasoning capabilities. In this work, we establish a comprehensive benchmark in the field of medical specialization and introduced RJUA-MedDQA, which contains 2000 real-world Chinese medical report images poses several challenges: comprehensively interpreting image content across a wide variety of challenging layouts, possessing the numerical reasoning ability to identify abnormal indicators and demonstrating robust clinical reasoning ability to provide the statement of disease diagnosis, status and advice based on a collection of medical contexts. We carefully design the data generation pipeline and proposed the Efficient Structural Restoration Annotation (ESRA) Method, aimed at restoring textual and tabular content in medical report images. This method substantially enhances annotation efficiency, doubling the productivity of each annotator, and yields a 26.8% improvement in accuracy. We conduct extensive evaluations, including few-shot assessments of 5 LMMs which are capable of solving Chinese medical QA tasks. To further investigate the limitations and potential of current LMMs, we conduct comparative experiments on a set of strong LMMs by using image-text generated by ESRA method. We report the performance of baselines and offer several observations: (1) The overall performance of existing LMMs is still limited; however LMMs more robust to low-quality and diverse-structured images compared to LLMs. (3) Reasoning across context and image content present significant challenges. We hope this benchmark helps the community make progress on these challenging tasks in multi-modal medical document understanding and facilitate its application in healthcare.

CCS CONCEPTS

• Computing methodologies → Machine Learning; • Information systems → Data mining; Data warehouses.

*Equal Contribution

†Yiran Huang is the corresponding author (huangyiran@renji.com)

‡Cong Fan is the corresponding author (fancong.fan@antgroup.com)

§Department of Urology, Shanghai Jiao Tong University School of Medicine Affiliated Renji Hospital

KEYWORDS

Large Multi-modal Model, Medical Dataset, Benchmark, Visual Question Answering, Medical Document Understanding, Contextual Reasoning

1 INTRODUCTION

The breakthroughs in large language models (LLMs) bring generalist AI models that can solve a wide range of medical challenges such as Automatic Diagnosis Agent [10, 20]. Large multi-modal models (LMMs) aim to achieve even stronger general intelligence via extending LLMs with multi-modal inputs such as Medical Imaging Analysis [24, 32]. Consequently, advances in Vision-Language multi-modal research can be beneficial in assisting in clinical decision-making, improving patient engagement, and helping relieve the burden of the healthcare system and improve medical professionals' efficiency [16].

Although these endeavors have led to remarkable strides forward, medical report understanding has received little attention so far, though it offers great potential for practical use since medical report images emerge as a powerful tool, offering a clear, concise, and accessible way to communicate vital clinical information including patient's basic information, examination details, abnormal test indicators and disease diagnosis. Generally, there are several available datasets with document-based VQA or reasoning-based VQA. Despite these important advances, limitations exist: (1) In currently available document-based datasets [8, 23, 27], most do not require reasoning ability. A few requires discrete reasoning based on image content such as TAT-DQA [35]. There is a lack of contextual reasoning dataset. (2) In currently available document VQAs and contextual-reasoning dataset, there are a lack of real-world medical visual document and specialized medical data relevant to diagnosis, status and advice of diseases. Meanwhile, the current LMM models still have trouble understanding information within a real-world image which usually diverse layout, skewed and blurry. Moreover, compared with humans, large LMMs are still not capable of performing numerical or contextual reasoning with successively logical connections within entire image. Based on these observations, we introduce a novel benchmark, RJUA-MedDQA, which are sampled from Shanghai Renji Hospital within Urology Department Database. The raw medical reports were subsequently processed and anonymized to create synthetic multi-modal clinical data for virtual patients, ensuring that no medical confidentiality or patient privacy is compromised. RJUA-MedDQA is designed to reflect the

challenges encountered in practice. We hope that this benchmark helps bridge the gap between academic research and practical scenarios to facilitate future study on multi-modal medical document understanding.

The dataset is collaboratively constructed by a team of urological experts from Shanghai Renji Hospital, comprising over 2,000 images of real-world medical report featuring a range of complex layouts that include both textual and tabular information, shown in Figure 1. RJUA-MedDQA is a high-level document understanding task wherein given a visually-rich medical report and a relevant question in natural language, and may attached with a set of facts or evidences extracted from official medical guideline or clinical experience. The model is required to give the correct answer to the question based on the image.

Our main contributions are summarized as follows:

- The Largest Medical Report Benchmark in Chinese:** RJUA-MedDQA is a comprehensive benchmark for visually-rich medical report understanding in Chinese, with a focus on Urology. To the best of our knowledge, this is also the largest real-world medical report VQA dataset. We decide to release a portion of the dataset with high-quality OCR results and annotations. Additionally, we define three tasks corresponding to different application scenarios. The primary goal of RJUA-MedDQA is to enhance LMMs to understand medical reports, enabling precise interpretation of content across varied diverse layouts and strong logical reasoning given a list of medical knowledge.
- Large Layout Variability:** The dataset comprises a variety of image types, including photographs, scanned PDFs, and screenshots that are not only characterized by their diverse and complex layouts from numerous public sources, but also by varying image quality. The photographed and screenshot images, in particular, may display signs of diminished quality due to factors, like rotation, skewing, blurriness of text, or missing information, highlighting challenges encountered in real-world scenarios.
- Efficient Structural Restoration Annotation (ESRA) Method:** In contrast to conventional layout annotation methods, we propose an efficient structure-aware labeling method to reconstruct both textual and tabular content in medical reports. It significantly reduces the human labeling errors and improves the efficiency of annotation process. Statistically, this method has elevated the accuracy rate from 70% to 96.8%.
- Synonym-aware Automatic QA Generator:** Given the ESRA method, we further integrated an synonym-aware automatic QA generator with an extensive range of templates, which are capable of handling tasks ranging from simple fact retrieval to more complex inference-based questions. Additionally, these templates are highly flexible to be customized based on given annotations, providing the capability to fine-tune or evaluate models on specialized research inquiries.
- Clinical Expert Annotation:** The dataset is also precisely annotated by urology specialists for contextual reasoning task. This dataset also provides an fact base, which includes logical chain on the diagnosis of disease and disease stage, and treatment advises, mainly extracted from clinical experience

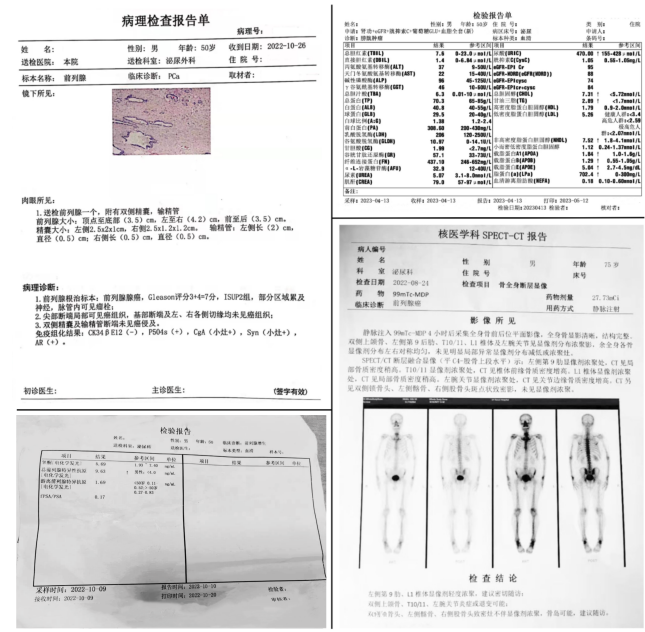


Figure 1: Complex Page Layouts in Various Medical Report Categories: Four Illustrative Examples

and official Urological Disease Diagnosis and Treatment Guide-line [12]. This fact base attempts to mitigate the gap between urological disease diagnosis and research communities.

2 RELATED WORK

In this section, we briefly review previous research in the datasets for Document VQA (DQA), reasoning over VQA and medical VQA, with special attention to those works that are most related to ours. The properties of these datasets and the comparison with ours are shown in Table 1.

Document VQA Document VQA is a high-level document understanding task wherein a model is required to answer a question in natural language given a visually-rich document. Some useful datasets have been published. DocVQA is constructed using various types of industry documents for extractive question answering, where answers can always be extracted from the text in the document [23]. VisualMRC dataset is built for abstractive question answering, where answers cannot be directly extracted from the text in the document [31]. Meanwhile, more datasets are moving beyond extractive question answering and are increasingly focusing on the reasoning capabilities over given image, including InfographicVQA [22], SlideVQA [30], TAT-DQA [35] and MultiModalQA [29]. All of these datasets require single-hop or multi-hop reasoning capabilities. Among them, InfographicVQA focuses on infographic instead of documents; SlideVQA focuses slide decks instead of documents; TAT-DQA dataset includes real-world high-quality business documents and MultiModalQA requires joint reasoning over textual and visual information in Wikipedia, while our RJUA-MedDQA dataset includes real-world medical documents of varying quality.

Table 1: Comparison of VQAs. Answer types can be broken down into single-span(SS), multi-span(MS), and non-span(NS). “S/P” denotes the “Scanned/Photographed” modality of images.

Dataset	Domain	#Images	Image Type	Images Modal Type	w/o Context Reasoning	w/ Context Reasoning	#QAs	Answer Type
DocVQA	General	12k	S	Document			50k	SS
TAT-DQA	Finance	2k	S	Document	✓		1.4k	SS,MS,NS
InfographicVQA	General	5k	S	Document	✓		30k	SS,MS,NS
SlideVQA	General	52k	S	Document	✓		14.5k	SS,MS,NS
MultiModalQA	General	57k	S	Document	✓		30k	SS,MS,NS
ScienceQA	General	6.5k	S	Non-document		✓	6.5k	NS
A-OKVQA	General	2.9k	S	Non-document		✓	2.9k	NS
SLAKE	Medical	642	S	Non-document	✓		14k	NS
RJUA-MedDQA	Medical	2k	S/P	Document	✓	✓	72k	SS,MS,NS

Contextual Reasoning VQA The previous task assumes that the datasets have a relevant image, containing all the facts required to answer. In Contextual Reasoning VQA task, the image may not have all the facts to answer a question. Instead, a rationale or a chunk of paragraph is given to provide the knowledge supplements each question: Context-VQA [25], ScienceQA [21] and A-OKVQA [28]. In Context-VQA, context refers to the type of website from which an image is sourced, which differs from our use of the term to describe additional data that aids in answering visual questions. Meanwhile, the context provided in ScienceQA is artificially-generated. However, all existing contextual Reasoning VQA contains visual or simple textual information but no layout information.

Medical VQA There are several public-available Medical VQA datasets up to date. VQA-MED-2018 [9], VQA-RAD [14], VQAMED-2019 [4], RadVisDial [13], PathVQA [11], VQA-MED-2020 [3], SLAKE [18], and VQA-MED-2021 [5]. The selected datasets are diverse in image modality and question categories. The imaging modality of those datasets covers chest X-ray, CT, MRI, and pathology. The questions include close-end questions and open-end questions on a variety of topics [17]. SLAKE is the most similar to us, as it is a comprehensive dataset with both semantic labels and a structural medical knowledge base. The medical knowledge base is presented as a knowledge graph, instead of being specific to each individual question. Furthermore, all these medical datasets comprise exclusively of visual image.

Therefore, we introduce RJUA-MedDQA for document-content understanding and contextual diagnosis reasoning. Our objective is to advance research in multi-modal document VQA within the academic community and to support the medical community in developing applications that improve their clinical reasoning abilities.

3 THE DATASET

3.1 Overview

The RJUA-MedDQA dataset contains a total of 2000 images, of which 402 are screenshot, 619 are scanned-PDF, and the remaining 979 are photos taken by patients during real-world medical consultations. Reports in screenshot and scanned-PDF format ensure the integrity and clarity of information; on the other hand, reports captured in photographs may exhibit some degree of quality degradation caused by issues such as rotated or skewed angles, blurred text, or incomplete information, which reveals real-world problems.

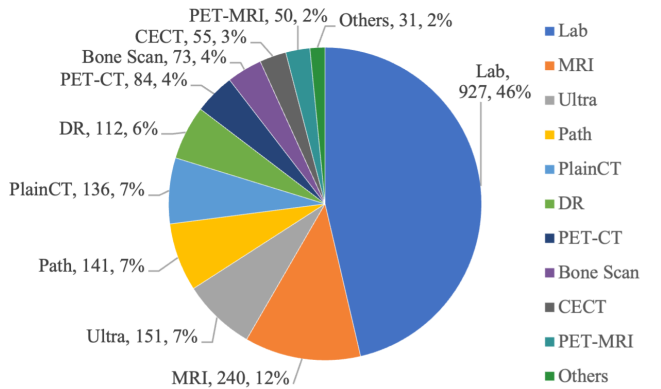


Figure 2: Statistics by report types

Medical reports can be grouped into two main categories, namely Laboratory Report and Clinical Report. Figure 2 shows the overall frequency and distribution of different report types.

Laboratory Reports: mainly include complete blood count (CBC), liver function tests (LFTs), urinalysis, and urological disease screening tests such as Prostate-Specific Antigen (PSA) Testing, which comprising a well-structured table and some relevant texts. Tables demonstrate large variability, ranging from single-column to multiple-column formats, with or without lines. Primarily, they convey laboratory results and its corresponding reference range.

Diagnostic Reports: mainly include MRI, Ultrasound, Pathology, Digital Radiography(DR), PlainCT, Contrast-enhanced CT (CECT), as well as other diagnostic modalities like PET-CT, PET-MRI, Endoscopy Report and Renogram.

Overall, the research team has compiled statistics for the year 2023, from Renji Hospital’s Department of Urology in Shanghai, encompassing initial diagnoses of urological diseases among 319,401 patients. They conducted 934,675 major laboratory tests, and a combined total of 401,615 examinations and pathological assessments. The dataset covers the top 50 most frequent laboratory tests to 95% (48/50) and the top 20 most frequent examinations and pathological procedures to 98% (18/20), respectively. Furthermore, the dataset covers over 334 different diseases and diagnoses, with detailed statistics provided in Appendix A. Characteristically, these reports

vary widely in their formatting, often including an extensive range of medical terminology and related synonyms, thereby achieving a high level of variability and the capacity for generalization.

3.2 Task Overview and Definition

We introduce RJUA-MedDQA dataset for the medical report understanding question-answering problem requiring models to possess the capability to interpret textual and tabular content within images, as well as reasoning capacity given a chunk of context. Consider a medical report D , which contains text content and possibly including a table, we propose two main tasks: (1) Non-Contextual QA in Report Comprehension; (2) Contextual QA in Clinical Reasoning.

3.2.1 Task 1: Non-Contextual QA in Report Comprehension. Given a question Q , the model \mathcal{F} is required to predict the answer a according to the report D . Formally, the task is formulated as

$$\mathcal{F}(D, Q) = a \quad (1)$$

In w/o context VQA, the answer may be either extracted from the given image, or generated by performing mathematical reasoning. To solve the former task, a LMM model needs to possess strong ability to interpret content and tabular layout in order to derive the final answer. In the second scenario, there is a demand for discrete reasoning capability across the entire visually-rich report.

3.2.2 Task 2: Contextual QA in Clinical Reasoning. Given a question Q , and a piece of context C that includes the gold facts necessary for answering Q and distracting facts, which is formulated as

$$\mathcal{F}(D, C, Q) = a \quad (2)$$

In w/ context VQA, the answer can be derived based on patient's basic information such as age, examination description and the evidence in the provided context. Questions include (1) Disease diagnosis based on abnormal indicators in laboratory report or examination findings in non-laboratory test report; (2) The current severity of the disease, such as staging of prostate cancer; (3) Definitive treatment advice. In this process, the capability of logical reasoning over the visual-language modality is much demanded.

4 DATA GENERATION PIPELINE

The Data Generation Pipeline was carried out in three phases. In phase one, we firstly identify and prepare the data sources, and then apply the Efficient Structural Restoration Annotation (ESRA) Method to structurally recovered textual and tabular content based on OCR results. In phase two, we carefully design the annotation guideline in order to obtain high efficiency and maximum consistency, and then upload each image along with its corresponding image-text to an online interface. The annotation process is mainly divided into two parts: 1) Image Content Annotation; 2) Clinical Reasoning Annotation. Both of them includes a efficient and detailed guideline with the format of the data, the specific labeling task and the examples of various types of labels. We performed continuous quality controls. In phase three, reviewed annotations are refined through an automated generator to produce the final dataset. A illustration is shown in Figure 3.

4.1 Efficient Structural Restoration Annotation

Given OCR results, the information of coordinates are converted to appropriate spaces and line breaks which connect all chunks of texts, resulting in structural text that is similar to the original medical report image(see Figure 4).

Mathematically, given a medical report image I , an OCR tool is applied to extract textual content. The resulting OCR results consist of extracted text segments and their corresponding bounding boxes (bbox) are denoted as $T = \{t_1, t_2, \dots, t_n\}$ and $B = \{b_1, b_2, \dots, b_n\}$, where n represents the number of text segments recognized.

Step 1 Based on the bbox $B = \{b_1, b_2, \dots, b_n\}$, partition the boxes that belong to the same text line. Specifically, the coordinates within B are sorted orderly from left to right, and then top to bottom, resulting new text segments $T^* = \{t_1^*, t_2^*, \dots, t_n^*\}$ and new bbox $B^* = \{b_1^*, b_2^*, \dots, b_n^*\}$, where $b_i^* = [x_{i,0}, x_{i,1}, y_{i,0}, y_{i,1}]$

Step 2 The bbox in B are traversed and converted into lines denoted as $line_i$ by line flag.

$$flag = \text{bool}[(y_{i+1,0} + \varepsilon_1 < \frac{y_{i,1} - y_{i,0}}{2}) \mid (y_{i,0} + \varepsilon_2 < \frac{y_{i+1,1} - y_{i+1,0}}{2} < y_{i,1} - \varepsilon_2)] \quad (3)$$

where $\varepsilon_1 = r^*(y_{i,1} - y_{i,0})$ and $\varepsilon_2 = r^*(y_{i+1,1} - y_{i+1,0})$. r^* is a discount coefficient ranging from 0 to 1. By setting this hyper-parameter r^* , the adhesion of text segments between lines can be mitigated, thereby increasing readability.

If $flag = \text{True}$, bbox b_i and b_{i+1} are on the same line.

If $flag = \text{False}$, a new line will be added, resulting bbox

$$B^* = \{line_1, line_2, \dots, line_n\} \quad (4)$$

where $line_i = \{b_{line_{i1}}^*, b_{line_{i2}}^*, \dots, b_{line_{in}}^*\}$.

Step 3 Define a set \mathcal{H} representing the heights of all bbox of $line_i$. Apply k-means clustering to \mathcal{H} on generate clusters. Within each cluster c_i , determine the character count N_i of bbox. Identify the cluster c_{max} that has the maximum character count. The total width of bbox within c_{max} is denoted as w_{total}^* and total characters in c_{max} is denoted as N_{total}^* . The average character width c^* can be calculated as:

$$c^* = \frac{w_{total}^*}{N_{total}^*} \quad (5)$$

Step 4 Join text segments in the same line by spaces. Given two adjacent text segments $b_{line_{ij}}^*, b_{line_{ik}}^*$

$$\text{number_of_spaces} = \max(\frac{h_{i,j,k}}{c^*l}, 1) \quad (6)$$

where $h_{i,j,k}$ is the horizontal distance between the bbox $b_{line_{ij}}^*, b_{line_{ik}}^*$. Additionally, l is an expansion coefficient from 0 to 1. By setting the hyper-parameter l , we control the coefficient that determines the number of spaces per line in the overall layout output, thereby increasing integrity.

A demonstration of the impact of different r on the output structure of ESRA method and detailed hyper-parameters setting can be found in Appendix B.1.

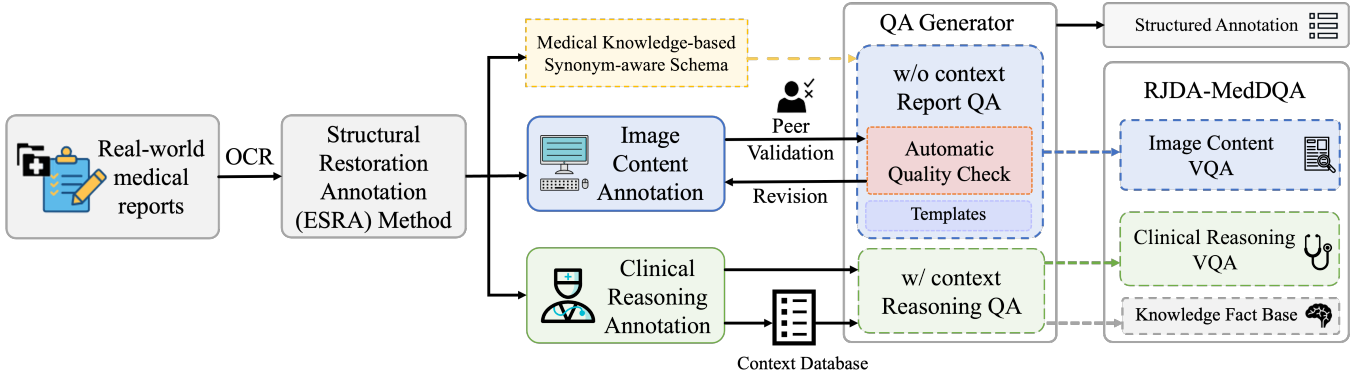


Figure 3: Data Generation Pipeline

Raw Laboratory Report Image			
姓名: [姓名]	性别: [性别]	年龄: [年龄]	住院号: [住院号]
项目: [项目]	结果: [结果]	参考区间: [参考区间]	类别: [类别]
项目: 肾功能C+胰岛素GLU+电解质+肝功能(新3)	结果: 51.80	参考区间: 1.05-4.20	类别: 血清
项目: 胆红素(TBL)	结果: 41.3	参考区间: 0-23.44 μmol/L	类别: 血清
直接胆红素(DBIL)	结果: 12.0	参考区间: 0-6.44 μmol/L	类别: 血清
丙氨酸氨基转移酶(ALT)	结果: 44	参考区间: 9-50U/L	类别: 血清
天门冬氨酸氨基转移酶(AST)	结果: 17	参考区间: 15-40U/L	类别: 血清
碱性磷酸酶(ALP)	结果: 44.1	参考区间: 30-120U/L	类别: 血清
γ-谷氨酰基转氨酶(GGT)	结果: 25	参考区间: 10-60U/L	类别: 血清
总胆红素(TTB)	结果: 0.8	参考区间: 0.01-10 μmol/L	类别: 血清
总蛋白(TP)	结果: 62.0	参考区间: 60-70 g/L	类别: 血清
白蛋白(ALB)	结果: 41.3	参考区间: 40-55g/L	类别: 血清
球蛋白(GLB)	结果: 20.7	参考区间: 20-40g/L	类别: 血清
白蛋白比(ALB/G)	结果: 2.00	参考区间: 1.2-2.4	类别: 血清
尿素(NH4)	结果: 283.0	参考区间: 200-400 mg/L	类别: 血清
谷氨酰胺(NH3)	结果: 4.95	参考区间: 0-14.1 μmol/L	类别: 血清
乳酸脱氢酶(LDH)	结果: 180	参考区间: 120-250U/L	类别: 血清
门冬氨酸氨基转移酶(GOT)	结果: 1.29	参考区间: 0-47U/L	类别: 血清
谷胱甘肽过氧化物酶(GSH-Px)	结果: 54.1	参考区间: 33-73U/L	类别: 血清
转铁蛋白(Tf)	结果: 315.70	参考区间: 246-652g/L	类别: 血清
转铁蛋白饱和度(Trf%)	结果: 20.6	参考区间: 12-40U/L	类别: 血清
转铁蛋白结合珠蛋白(AfU)	结果: 4.46	参考区间: 3.1-4.0 mmol/L	类别: 血清
肌酐(crea)	结果: 82.0	参考区间: 57-97 μmol/L	类别: 血清

Arranged Bounding Boxes from ESRA

Line 1: [[54, 103, 115, 132], [370, 103, 455, 132], [481, 104, 691, 127], [938, 103, 1017, 130]]]	
Text 1: [姓名: '性别: 男', 年龄: '26岁', 住院号: '']	
Line 2: [[60, 134, 562, 151], [599, 132, 693, 155], [941, 131, 1015, 153]]]	
Text 2: [申请: '肾功能+胱抑素C+葡萄糖GLU+电解质+肝功能(新3)', '病区床号: ']	
Line 10: [[63, 336, 272, 356], [398, 336, 427, 360], [513, 336, 716, 358], [918, 336, 1145, 357]]]	
Text 10: [谷氨酰基转氨酶(GGT), '25', '10-60U/L', 葡萄糖(GLU), '14.04', '3.9-6.1mmol/L']	
Line 24: [[53, 675, 160, 705], [378, 679, 426, 703], [470, 679, 597, 703]]]	
Text 24: [肌酐(crea), '82.0', '57-97μmol/L']	

Structural Recovery Text	
姓名: [姓名]	性别: [性别]
项目: [项目]	年龄: [年龄]
申请: [申请]	住院号: [住院号]
类别: [类别]	申请人: [申请人]
诊断: 肾功能+胱抑素C+葡萄糖GLU+电解质+肝功能(新3)	标本种类: 血清
结果: 参考区间	结果: 参考区间
总胆红素(TBL)	结果: 41.3, 参考区间: 0-23.44 μmol/L
直接胆红素(DBIL)	结果: 12.0, 参考区间: 0-6.44 μmol/L
丙氨酸氨基转移酶(ALT)	结果: 44, 参考区间: 9-50U/L
天门冬氨酸氨基转移酶(AST)	结果: 17, 参考区间: 15-40U/L
碱性磷酸酶(ALP)	结果: 44, 参考区间: 45-125U/L
γ-谷氨酰基转氨酶(GGT)	结果: 25, 参考区间: 10-60U/L
总蛋白(TP)	结果: 62.0, 参考区间: 60-70 g/L
白蛋白(ALB)	结果: 41.3, 参考区间: 40-55g/L
球蛋白(GLB)	结果: 20.7, 参考区间: 20-40g/L
白蛋白比(ALB/G)	结果: 2.00, 参考区间: 1.2-2.4
尿素(NH4)	结果: 283.0, 参考区间: 200-400 mg/L
谷氨酰胺(NH3)	结果: 4.95, 参考区间: 0-14.1 μmol/L
乳酸脱氢酶(LDH)	结果: 180, 参考区间: 120-250U/L
门冬氨酸氨基转移酶(GOT)	结果: 1.29, 参考区间: 0-47U/L
谷胱甘肽过氧化物酶(GSH-Px)	结果: 54.1, 参考区间: 33-73U/L
转铁蛋白(Tf)	结果: 315.70, 参考区间: 246-652g/L
转铁蛋白饱和度(Trf%)	结果: 20.6, 参考区间: 12-40U/L
转铁蛋白结合珠蛋白(AfU)	结果: 4.46, 参考区间: 3.1-4.0 mmol/L
肌酐(crea)	结果: 82.0, 参考区间: 57-97 μmol/L

Figure 4: A Demonstration of ESRA method

4.2 Annotation Process

All images are uploading to a online platform which provides a visual annotation interface and allows for dataset inspection and analysis.

4.2.1 Image Content Annotation. A group of 10 dedicated annotators with basic medical knowledge were responsible for this part to ensure the accuracy and professionalism of data labeling. We review the collected reports, identify the most common structural features they exhibit, and choose two most representative aspects:

- Key-Value Pairs: Annotators are required to identify and extract key information pairs from images, such as age, examination date, pre-examination clinical diagnosis findings, etc., and label them as structured fields.
- Quadruplets <item, result, range, is_abnormal> Annotators are required to restoring the structure of tables, including the name of item and the corresponding result and reference interval, and mark abnormality. Each indicator can be labeled as normal, abnormal, or undetermined—the latter if no reference range is given. For abnormal results, annotators must also specify if the value is high or low.

All contents in the report image are annotated either Key:value pairs or Quadruplets. During the labeling process, annotators need to appropriately fill incomplete information such as the missing keys and partially missing item names to increase the generalization ability of the dataset.

Overall, ESRA approach greatly diminishes the possibility of human input errors and enhances the efficiency of annotation. It avoids the use of traditional typing by annotators, significantly reducing the error rate that may occur during the typing process and saving huge amount of time for typing obscure medical terminology and descriptions. Additionally, annotators also refine OCR results to further improve accuracy. Consequently, the work efficiency of the standard annotators can be increased from 5 images per hour to 10 images per hour. The accuracy rate has improved from 70% to 96.8% by manually inspecting the annotation quality of 100 images.

4.2.2 Quality Check. The production phase took around three weeks to complete. Subsequently, a peer-validation was carried out to rectify any errors in the annotations. We further conducted continuous quality checks during data QA generation process by designing an automated quality check tool based on this annotation framework. It includes features to identify issues such as missing keys or values, discrepancies in the number of table items, and the potential for error in the assessment of abnormal indicators. Problematic samples are returned for re-verification and manual annotation correction.

4.2.3 Clinical Reasoning Annotation. A small team of 5 urological experts are assembled for Clinical Reasoning Annotation. It is more time-consuming even with the assistance of ESRA, because it demands the specialized knowledge and clinical experience. To accelerate this process and streamline the subsequent generation

Table 2: Examples of QA generators for a variety of task and difficulties (*Synonyms*) Annotations

Task	Sub-task	Question Template	Answer Template
Entity	Single	What is key (<i>impression</i>)?	key is value.
	Multi	What are key1 (<i>age</i>) and key2 (<i>date</i>)?	value1; value2
Table	Single Cell	What is the (<i>laboratory result</i>) of item1	The (<i>laboratory result</i>) of item1 is result1.
	Single Row	What is the (<i>result</i>) and (<i>reference range</i>) of item1 ?	The (<i>result</i>) of item1 is result1, and the (<i>reference range</i>) is range1.
	Multi-Row	What are the (<i>results</i>) and (<i>standard interval</i>) of item1 and item2 correspondingly?	item1, result1, range1; item2, result2, range2;
TableNR	Comparison	Is item1 within (<i>normal range</i>)?	The (<i>result</i>) of item1 is result1 and the (<i>normal range</i>) is range1, hence is_abnormal1
	Multi	Is there any (<i>abnormal indicators</i>) in this report?	is_abnormal1, is_abnormal3, is_abnormal9.
Customized	Summarization	What key elements should be noticed in this medical report?	There are len([items]) in this report. len(is_abnormal==1) are not in standard reference, which are ...

of the QA dataset, we firstly established a context database. Meanwhile, in order to mirror the real-world diagnostic process of doctors reviewing reports, context are categorized into: 1) Examination-Disease 2) Examination-Status; 3) Disease-Status; 4) Disease-Advice; 5) Examination; 6) Disease-Examination 7) Disease-Treatment.

In this way, physicians can add relevant context directly to the database while annotating, by indexing each context a descriptive title. They can quickly reference and tag recurring content, significantly boosting annotation efficiency and consistency.

Consequently, the labeling of each report involves assigning context indexes for: 1) Diagnosis; 2) Staging or status; and 3) Advice, treatment or supplementary examinations. All labeling statements are unambiguous and unbiased, and all suspicious findings are excluded. A report may contain none, one or more diagnoses, which may be explicitly displayed in report, or could be inferred from the report content and corresponding context. Statistics, analysis and detailed examples of annotated contexts are shown in Appendix B.2 (see Table 8).

4.3 VQA Generation

We propose a KG-based schema Question-Answering (QA) generator based on the structurally annotation format, as shown in Section 4.2.3.

4.3.1 Medical Knowledge-based Synonym-aware Schema. Reports from different healthcare information systems often employ various forms of expression, and these differences tend to be further amplified in the Chinese medical terminology. For instance, the presentation of test results in non-laboratory test reports might vary, being described as “impressions”, “pathological diagnosis” or “conclusions”; similarly, reference intervals in laboratory test reports might be referred to as “normal ranges”, “normal intervals” or “standard values”. To reduce the complexity of parsing annotation results, and to increase the diversity of question-asking templates, we have analyzed all the keys from annotations. Together urological experts, we construct a knowledge-based schema that integrates the validated list of synonyms into a comprehensive framework, which includes common vocabulary and their synonyms from different types of reports. Based on this schema, data mapping can be easily performed resulting not only a reduction in ambiguity and errors associated with the interpretation of medical reports due

to synonym usage, and an increase in diversity during question generation process to enhanced data interoperability.

4.3.2 VQA Generator.

In RJUA-MedDQA dataset, we proposed two tasks: Image Content VQA and Clinical Reasoning VQA.

Image Content VQA Generation: This task includes entity-based and tabular-based VQA and requires no contextual information. The core of the w/o Content VQA Generation is task generators. Each generator corresponding to multiple sub-task question templates, which differ in their difficulties shown in Table 2. Templates contain annotated variables from reports, and (*vocabulary*) in synonym schema. Employing these templates, we generate questions of varying difficulty, which can be enriched through annotations to include complex queries involving dual entities, single-row or multi-row questions. During the formulation of questions, we employ synonym substitution to enhance the generalization ability of our dataset. we have designed templates grounded in our schema and the specific annotation format.

Customization: In addition to existing QA pairs in the dataset, we provide key-value pair annotations and quadruplets, enabling the construction of customized templates to meet diverse model requirements such as summarization task shown in Table 2.

Clinical Reasoning VQA Generation: This task includes multiple choice (MC) and short-answer questions (SA). In each report, diagnosis, status or advice may be explicitly displayed, or could be inferred from image content and corresponding context. For latter one, we match the title from context fact base and use bert-base-chinese [7] embedding and cosine similarity to find the top three similar titles to be distracting options. We have evenly distributed the proportion of each option in the question bank. The answers to the short-answer questions consist of one or more of the correct answers from multiple-choice questions.

5 EXPERIMENTS

In this section, we report and analyze the extensive experimental results to demonstrate the validity of RJUA-MedDQA.

5.1 Baseline Models

There are very limited LMM models that have been proposed to effectively solve Chinese medical QA tasks over the images containing

Table 3: Performance of Baseline Models on RJUA-MedDQA. Best results are marked in bold

Method		Image Content					Clinical Reasoning	
		Entity		Table		TableNR	MC	SA
		RougeL	Acc	RougeL	Acc	Acc	Acc	RougeL
LMMs	LLaVA-v1.5-7B	0.08	0.04	0.08	0.04	0.36	0.15	0.11
	mPLUG-Owl2-9.8B	0.17	0.09	0.22	0.02	0.31	0.28	0.13
	Qwen-VL-Chat-9.6B	0.28	0.20	0.28	0.14	0.33	0.30	0.11
	Qwen-VL-Plus-[API]	0.46	0.51	0.38	0.53	0.52	0.32	0.15
	GPT-4v-[API]	0.45	0.38	0.68	0.47	0.50	0.46	0.23
ImageText+ LLMs	ESRA+Qwen-[API]	0.77	0.80	0.50	0.73	0.68	0.66	0.18
	ESRA+GPT-4-[API]	0.79	0.76	0.62	0.72	0.63	0.79	0.29

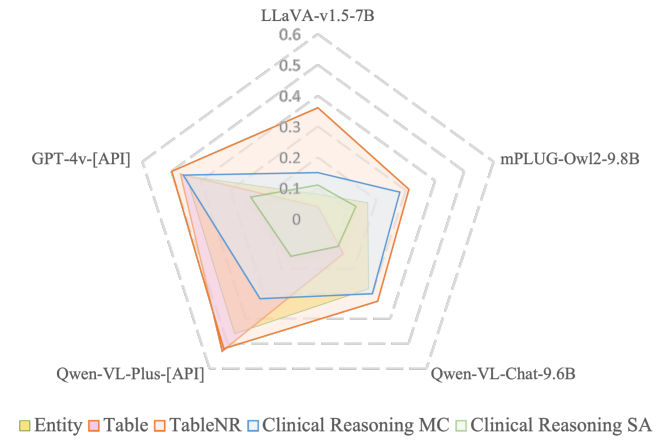
both tabular data and textual, where contextual reasoning ability is particularly demanded. We select 5 different multi-modality models and benchmark them on the dataset. The models we have selected cover a broad spectrum of strategies and architectures, effectively illustrating the current state-of-the-art in multimodal understanding i.e. LLaVA-v1.5-7B [19], mPLUG-Owl2-9.8B [34], Qwen-VL-Chat-9.6B, Qwen-VL-Plus-[API] [2] and GPT-4v-[API] [33]. In addition to LMMs, we conduct comparative experiments on a set of strong LLMs by using image-text generated by ESRA method to further investigate the limitations and potential of current LMMs. We will use Qwen-[API] [1] and GPT-4-[API] [26] for this purpose.

5.2 Evaluation metrics

The dataset includes diverse tasks which are framed as either short-answer questions or single-choice questions. Our observations indicate that LMMs exhibit preferences for specific answering techniques. For instance, when providing short answers, LMMs tend to rephrase the question before presenting their response. In the case of single-choice questions, the models frequently produce a complete sentence that either corresponds directly with one of the options or is semantically similar to it, sometimes even accompanied by an explanation. Consequently, the reliance on a single evaluation metric or merely comparing the similarity between the model-generated answers and the ground truth (ANLS [6]) can potentially amplify biases in assessment. Therefore, to achieve a more fair evaluation, we have implemented task-specific metrics within the dataset, which allows us to capture the distinct nuances of LMM performance. For Table Numerical Reasoning (NR) QA and Clinical Reasoning Multiple Choice (MC), we adopt soft accuracy which means the predict answer is considered to be correct if it contains the ground truth. For Entity QA, Table QA and Clinical Reasoning Short Answer(SA), we will report both soft accuracy and ROUGE-L [15] for comparison.

5.3 Results and Analysis

5.3.1 Overall Results. We exhaustively evaluate the five models on the existing 5 sub-tasks of RJUA-MedDQA. In Table 3, we present the models' overall performance on various QA tasks namely Entity, Table, NR, Clinical Reasoning MC and SA. Among five LMMs, Qwen-VL-Plus and GPT-4v yield superior results on all tasks, while LLaVA-v1.5-7B and mPLUG-Owl2 demonstrate lower overall performance on Chinese VQA tasks compared to the other models. The performance patterns of Qwen-VL-Plus and GPT-4v on Entity

**Figure 5: Results of 5 LMMs across 5 tasks**

and Table tasks are intriguingly divergent when evaluated using two metrics. One explanation is that Qwen often deviates from the prompt instructions, resulting in longer sentences that negatively impact its RougeL score; while GPT4v tends to change output format such as the decimal place of floats, leading to lower accuracy but higher RougeL score. However, both responses are generally accurate. For entities, where longer text is involved, we prefer to rely on RougeL, while for tables, we opt for Soft Accuracy as a reference. Overall, Qwen-VL-Plus is more proficient in image-content related QAs; while GPT4v shows stronger in-context reasoning ability and perform the best in Clinical Reasoning Tasks.

Compared to LMMs, ESRA+LLMs yields superior results so far. ESRA+GPT4's performance on most tasks is far better than that of LMMs. Meanwhile, the performance of all models in Clinical Reasoning SA is not satisfactory.

5.3.2 Impact of Image Quality. For a more in-depth understanding, we provide a comprehensive analysis of the image type (Electronic vs Photo see Table 9) and photo quality (High vs Low) on model performance. Although the capabilities of current LMMs are still quite limited and not outperforming traditional image-text with LLMs, an interesting fact emerged when analyzing the impact of image quality on model performance on tabular content (Table 4). LMMs are more robust to low-quality and diverse-structured images. Table QA requires high image quality since because even minor levels

of distortion can lead to a significant drop in model performance. The disparity in GPT-4's ability to process tables is highlighted by a significant performance gap, approximately 0.3, between high and low-quality images, whereas the gap is 0.22 in Qwen. In contrast, such a stark difference in performance is not observed in LMMs. A similar trend is observed when comparing the handling of electronic images and photos. Overall, LMMs often exhibit enhanced performance even with low-quality images, suggesting a level of robustness inherent to multi-modal methodologies that uni-modal OCR-based models may not possess. In Appendix C.3, we present several cases of low-quality images that demonstrate robustness to quality degradation (Figure 9).

5.3.3 Clinical Reasoning. Studies indicates that the existence of context definitely improves model performance (Table 11). However, the evaluation results reveals that cross-instance understanding and logic reasoning pose a significant challenge for existing LMMs (Table 5). GPT-4v exhibits the most advanced reasoning capabilities among all LMMs, yet it falls notably behind ESRA+GPT4 by approximately 0.3. This pattern is mirrored in the comparison between QwenVL+ and QwenVL+ESRA, with an even larger gap of 0.45. It is observed that disease diagnosis tends to be a less complex task than providing clinical advice in table reasoning tasks, as the latter demands multi-step reasoning - a challenge evidently not met by any model except for ESRA+GPT-4. Meanwhile, the SA performance for laboratory and clinical diagnosis by existing models is remarkably poor, with the highest RougeL score being only 0.33. The results indicate that improving the medical report understanding and contextual reasoning capabilities of LLMs can be a significant and promising direction.

5.4 Case study

We visualize several loss cases in the experiments of GPT-4v and Qwen-VL-Plus in Appendix C.3. We hope this provide inspirations for future improvements.

Incorrect Extraction A large portion of errors are caused by incorrect extraction, an issue that frequently occurs in table QA. For instance, failing to find the correct item name can lead to mistakes when getting reference ranges. A subset of these errors is due to incomplete extraction, where the model correctly identifies the correct entity but fails to include all the necessary information. It's especially hard for models to correctly extract longer text that spans multiple lines (see Figure 10).

Hallucination is another common issue, where the model confidently generates text that is not present in the image. We randomly selected 84 questions in Entity QA and 50 questions in Table QA that are unanswerable. Statistics show that models exhibit hallucination issues to varying degrees, with LMMs facing more severe problems. For instance, in Entity Tasks, GPT-4v produced incorrect responses for 54 out of 84 questions; in Table Tasks, the error rate was 35 out of 50 (see Figure 10, Figure 8).

Faulty Reasoning Compared to LLMs, LMMs also need to initially locate the correct content, which adds a certain level of difficulty. (see Figure 11, Figure 13) In SA tasks, with no hint from options, models are tend to extract text that is directly relevant to the imagery's semantics, rather than fully understanding the test description, conclusions, and corresponding context. For instance,

Table 4: Impact of Photo Quality on Model Performance

Method	Entity		Table		TableNR	
	High		Low		High	
	RougeL	RougeL	Acc	Acc	Acc	Acc
LLaVA-v1.5	0.08	0.07	0.03	0.06	0.39	0.38
mPLUG-Owl2	0.19	0.08	0.02	0.01	0.27	0.21
Qwen-VL-Chat	0.33	0.29	0.08	0.09	0.33	0.26
Qwen-VL-Plus	0.47	0.42	0.35	0.36	0.44	0.40
GPT-4v	0.51	0.44	0.46	0.34	0.48	0.39
ESRA+Qwen	0.83	0.79	0.75	0.58	0.70	0.52
ESRA+GPT-4	0.82	0.77	0.71	0.40	0.61	0.48

Table 5: Performance of Baseline Models on Clinical Reasoning. "D", "S", "A" denotes the "Disease", "Status", "Advice"

Method	Multiple Choice				Short Answer			
	Table		Clinical		Table		Clinical	
	D	Ad	S	A	D	A	S	A
LLaVA-v1.5	0.1	0.13	0	0.05	0.14	0.07	0.17	0.01
mPLUG-Owl2	0.18	0.17	0	0.27	0.1	0.03	0.01	0.00
Qwen-VL-Chat	0.24	0.21	0	0.29	0.1	0	0.01	0.01
Qwen-VL-Plus	0.3	0.25	0.25	0.33	0.11	0.02	0.01	0.01
GPT-4v	0.5	0.47	0.33	0.59	0.21	0.02	0.19	0.04
ESRA+Qwen	0.75	0.65	0.33	0.52	0.06	0	0.1	0.04
ESRA+GPT-4	0.86	0.87	0.5	0.67	0.22	0.05	0.33	0.06

taking the phrase "pre-clinical diagnosis" as the diagnosis for the entire report (see Figure 12). Qwen exhibits the same issue, leading to a even inferior performance to GPT-4v.

6 CONCLUSION AND FUTURE STUDY

In this paper, we introduce a new benchmark RJUA-MedDQA to measure progress on image content extractions and clinical reasoning from visually-rich medical documents in real application. We also proposed a comprehensive data generation pipeline including a image-text restoration method, thoughtful annotation guideline and automatic QA generator which significantly improves efficiency and accuracy. The evaluation results reveals that LMMs demonstrate robustness to quality poor-quality images but still struggle with complex reasoning tasks involving cross-instance understanding and strong logical link. Our research aims to help improve multi-modal understanding of medical documents and aid in healthcare applications. In future study, We will also focus on the three areas of opportunity discovered in this paper, and explore approaches that can improves contextual reasoning tasks.

REFERENCES

[1] Jinze Bai, Shuai Bai, Yunfei Chu, Zeyu Cui, Kai Dang, Xiaodong Deng, Yang Fan, Wenbin Ge, Yu Han, Fei Huang, Binyuan Hui, Luo Ji, Mei Li, Junyang Lin, Runji Lin, Dayiheng Liu, Gao Liu, Chengqiang Lu, Keming Lu, Jianxin Ma, Rui Men, Xingzhang Ren, Xuancheng Ren, Chuanqi Tan, Sinan Tan, Jianhong Tu, Peng Wang, Shijie Wang, Wei Wang, Shengguang Wu, Benfeng Xu, Jin Xu, An Yang, Hao Yang, Jian Yang, Shusheng Yang, Yang Yao, Bowen Yu, Hongyi Yuan, Zheng Yuan, Jianwei Zhang, Xingxuan Zhang, Yichang Zhang, Zhenru Zhang, Chang Zhou, Jingren Zhou, Xiaohuan Zhou, and Tianhang Zhu. 2023. Qwen Technical Report. arXiv:2309.16609 [cs.CL]

[2] Jinze Bai, Shuai Bai, Shusheng Yang, Shijie Wang, Sinan Tan, Peng Wang, Junyang Lin, Chang Zhou, and Jingren Zhou. 2023. Qwen-VL: A Versatile Vision-Language Model for Understanding, Localization, Text Reading, and Beyond. [arXiv:2308.12966 \[cs.CV\]](https://arxiv.org/abs/2308.12966)

[3] Asma Ben Abacha, Vivek V. Datla, Sadid A. Hasan, Dina Demner-Fushman, and Henning Müller. 2020. Overview of the VQA-Med Task at ImageCLEF 2020: Visual Question Answering and Generation in the Medical Domain. In *CLEF 2020 Working Notes (CEUR Workshop Proceedings)*. CEUR-WS.org <<http://ceur-ws.org/>>, Thessaloniki, Greece.

[4] Asma Ben Abacha, Sadid A. Hasan, Vivek V. Datla, Joey Liu, Dina Demner-Fushman, and Henning Müller. 2019. VQA-Med: Overview of the Medical Visual Question Answering Task at ImageCLEF 2019. In *Working Notes of CLEF 2019 (CEUR Workshop Proceedings, Vol. 2380)*. CEUR-WS.org, Lugano, Switzerland. https://ceur-ws.org/Vol-2380/paper_272.pdf

[5] Asma Ben Abacha, Mourad Sarouti, Dina Demner-Fushman, Sadid A. Hasan, and Henning Müller. 2021. Overview of the VQA-Med Task at ImageCLEF 2021: Visual Question Answering and Generation in the Medical Domain. In *CLEF 2021 Working Notes (CEUR Workshop Proceedings)*. CEUR-WS.org, Bucharest, Romania.

[6] Ali Furkan Biten, Rubén Tito, Andres Mafla, Lluís Gomez, Marçal Rusiñol, Minesh Mathew, C. V. Jawahar, Ernest Valveny, and Dimosthenis Karatzas. 2019. ICDAR 2019 Competition on Scene Text Visual Question Answering. [arXiv:1907.00490 \[cs.CV\]](https://arxiv.org/abs/1907.00490)

[7] Jacob Devlin, Ming-Wei Chang, Kenton Lee, and Kristina Toutanova. 2019. BERT: Pre-training of Deep Bidirectional Transformers for Language Understanding. [arXiv:1810.04805 \[cs.CL\]](https://arxiv.org/abs/1810.04805)

[8] Yihao Ding, Siwen Luo, Hyunsuk Chung, and Soyeon Caren Han. 2023. PDFVQA: A New Dataset for Real-World VQA on PDF Documents. [arXiv:2304.06447 \[cs.CV\]](https://arxiv.org/abs/2304.06447)

[9] Sadid A. Hasan, Yuan Ling, Oladimeji Farri, Joey Liu, Henning Müller, and Matthew P. Lungren. 2018. Overview of ImageCLEF 2018 Medical Domain Visual Question Answering Task. In *Conference and Labs of the Evaluation Forum*. <https://api.semanticscholar.org/CorpusID:51943124>

[10] Kai He, Rui Mao, Qika Lin, Yucheng Ruan, Xiang Lan, Mengling Feng, and Erik Cambria. 2023. A Survey of Large Language Models for Healthcare: from Data, Technology, and Applications to Accountability and Ethics. [arXiv:2310.05694 \[cs.CL\]](https://arxiv.org/abs/2310.05694)

[11] Xuehai He, Yichen Zhang, Luntian Mou, Eric Xing, and Pengtao Xie. 2020. PathVQA: 30000+ Questions for Medical Visual Question Answering. [arXiv:2003.10286 \[cs.CL\]](https://arxiv.org/abs/2003.10286)

[12] Xu Zhang Jian Huang. 2022. Chinese Urological and Andrological Diseases Diagnosis and Treatment Guidelines: 2022 Edition.

[13] Olga Kovaleva, Chaitanya Shivade, Satyananda Kashyap, Karina Kanjaria, Joy Wu, Deddeh Ballah, Adam Coy, Alexandros Karargyris, Yufan Guo, David Beyer Beymer, Anna Rumshisky, and Vandana Mukherjee Mukherjee. 2020. Towards Visual Dialog for Radiology. In *Proceedings of the 19th SIGBioMed Workshop on Biomedical Language Processing*. Dina Demner-Fushman, Kevin Bretonnel Cohen, Sophia Ananiadou, and Junichi Tsuji (Eds.). Association for Computational Linguistics, Online, 60–69. <https://doi.org/10.18653/v1/2020.bionlp-1.6>

[14] Jason J. Lau, Soumya Gayen, Asma Ben Abacha, and Dina Demner-Fushman. 2018. A dataset of clinically generated visual questions and answers about radiology images (*Scientific Data*, Vol. 180251). <https://doi.org/10.1038/sdata.2018.251>

[15] Chin-Yew Lin. 2004. ROUGE: A Package for Automatic Evaluation of Summaries. In *Text Summarization Branches Out*. Association for Computational Linguistics, Barcelona, Spain, 74–81. <https://aclanthology.org/W04-1013>

[16] Zhihong Lin, Donghao Zhang, Qingyi Tao, Danli Shi, Gholamreza Haffari, Qi Wu, Mingguang He, and Zongyuan Ge. 2023. Medical visual question answering: A survey. *Artificial Intelligence in Medicine* 143 (Sept. 2023), 102611. <https://doi.org/10.1016/j.artmed.2023.102611>

[17] Zhihong Lin, Donghao Zhang, Qingyi Tao, Danli Shi, Gholamreza Haffari, Qi Wu, Mingguang He, and Zongyuan Ge. 2023. Medical visual question answering: A survey. *Artificial Intelligence in Medicine* 143 (Sept. 2023), 102611. <https://doi.org/10.1016/j.artmed.2023.102611>

[18] Bo Liu, Li-Ming Zhan, Li Xu, Lin Ma, Yan Yang, and Xiao-Ming Wu. 2021. SLAKE: A Semantically-Labeled Knowledge-Enhanced Dataset for Medical Visual Question Answering. [arXiv:2102.09542 \[cs.CV\]](https://arxiv.org/abs/2102.09542)

[19] Haotian Liu, Chunyu Li, Yuheng Li, and Yong Jae Lee. 2023. Improved Baselines with Visual Instruction Tuning. [arXiv:2310.03744 \[cs.CV\]](https://arxiv.org/abs/2310.03744)

[20] Wenge Liu, Yi Cheng, Hao Wang, Jianheng Tang, Yafei Liu, Ruihui Zhao, Wenjie Li, Yefeng Zheng, and Xiaodan Liang. 2022. "My nose is running." "Are you also coughing?": Building A Medical Diagnosis Agent with Interpretable Inquiry Logics. [arXiv:2204.13953 \[cs.CL\]](https://arxiv.org/abs/2204.13953)

[21] Pan Lu, Swaroop Mishra, Tony Xia, Liang Qiu, Kai-Wei Chang, Song-Chun Zhu, Oyvind Tafjord, Peter Clark, and Ashwin Kalyan. 2022. Learn to Explain: Multimodal Reasoning via Thought Chains for Science Question Answering. [arXiv:2209.09513 \[cs.CL\]](https://arxiv.org/abs/2209.09513)

[22] Minesh Mathew, Viraj Bagal, Rubén Pérez Tito, Dimosthenis Karatzas, Ernest Valveny, and C. V Jawahar. 2021. InfographicVQA. [arXiv:2104.12756 \[cs.CV\]](https://arxiv.org/abs/2104.12756)

[23] Minesh Mathew, Dimosthenis Karatzas, and C. V. Jawahar. 2021. DocVQA: A Dataset for VQA on Document Images. [arXiv:2007.00398 \[cs.CV\]](https://arxiv.org/abs/2007.00398)

[24] Jong Hak Moon, Hyungyung Lee, Woncheol Shin, Young-Hak Kim, and Edward Choi. 2022. Multi-Modal Understanding and Generation for Medical Images and Text via Vision-Language Pre-Training. *IEEE Journal of Biomedical and Health Informatics* 26, 12 (Dec. 2022), 6070–6080. <https://doi.org/10.1109/jbhi.2022.3207502>

[25] Nandita Naik, Christopher Potts, and Elisa Kreiss. 2023. Context-VQA: Towards Context-Aware and Purposeful Visual Question Answering. [arXiv:2307.15745 \[cs.CL\]](https://arxiv.org/abs/2307.15745)

[26] OpenAI. 2023. GPT-4 Technical Report. [arXiv:2303.08774 \[cs.CL\]](https://arxiv.org/abs/2303.08774)

[27] Birgit Pfitzmann, Christoph Auer, Michele Dolfi, Ahmed S. Nassar, and Peter Staar. 2022. DocLayNet: A Large Human-Annotated Dataset for Document-Layout Segmentation. In *Proceedings of the 28th ACM SIGKDD Conference on Knowledge Discovery and Data Mining (KDD '22)*. ACM. <https://doi.org/10.1145/3534678.3539043>

[28] Dustin Schwenk, Apoorv Khandelwal, Christopher Clark, Kenneth Marino, and Roozbeh Mottaghi. 2022. A-OKVQA: A Benchmark for Visual Question Answering using World Knowledge. [arXiv:2206.01718 \[cs.CV\]](https://arxiv.org/abs/2206.01718)

[29] Alon Talmor, Ori Yoran, Aminon Catav, Dan Lahav, Yizhong Wang, Akari Asai, Gabriel Ilharco, Hannaneh Hajishirzi, and Jonathan Berant. 2021. MultiModalQA: Complex Question Answering over Text, Tables and Images. [arXiv:2104.06039 \[cs.CL\]](https://arxiv.org/abs/2104.06039)

[30] Ryota Tanaka, Kyosuke Nishida, Kosuke Nishida, Taku Hasegawa, Itsumi Saito, and Kuniko Saito. 2023. SlideVQA: A Dataset for Document Visual Question Answering on Multiple Images. [arXiv:2301.04883 \[cs.CL\]](https://arxiv.org/abs/2301.04883)

[31] Ryota Tanaka, Kyosuke Nishida, and Sen Yoshida. 2021. VisualMRC: Machine Reading Comprehension on Document Images. [arXiv:2101.11272 \[cs.CL\]](https://arxiv.org/abs/2101.11272)

[32] Li Xu, Bo Liu, Ameer Hamza Khan, Lu Fan, and Xiao-Ming Wu. 2023. Multi-modal Pre-training for Medical Vision-language Understanding and Generation: An Empirical Study with A New Benchmark. [arXiv:2306.06494 \[cs.CV\]](https://arxiv.org/abs/2306.06494)

[33] Zhengyuan Yang, Linjie Li, Kevin Lin, Jianfeng Wang, Chung-Ching Lin, Zicheng Liu, and Lijuan Wang. 2023. The Dawn of LMMs: Preliminary Explorations with GPT-4V(ision). [arXiv:2309.17421 \[cs.CV\]](https://arxiv.org/abs/2309.17421)

[34] Qinghao Ye, Haiyang Xu, Jiaob Ye, Ming Yan, Anwen Hu, Haowei Liu, Qi Qian, Ji Zhang, Fei Huang, and Jingren Zhou. 2023. mPLUG-Owl2: Revolutionizing Multi-modal Large Language Model with Modality Collaboration. [arXiv:2311.04257 \[cs.CL\]](https://arxiv.org/abs/2311.04257)

[35] Fengbin Zhu, Wenqiang Lei, Fuli Feng, Chao Wang, Haozhou Zhang, and Tat-Seng Chua. 2022. Towards Complex Document Understanding By Discrete Reasoning. In *Proceedings of the 30th ACM International Conference on Multimedia (MM '22)*. ACM. <https://doi.org/10.1145/3503161.3548422>

A STATISTICS OF IMAGE

The RJUA-MedDQA dataset comprises 2000 images, among which 402 are screenshots, 619 are scanned PDFs, and the remaining 979 are photos taken by patients in real-world medical consultations. Within the photos category, we classified each image based on its quality. The evaluation of low-quality images is dependent on two sensors: Completeness Sensor and Angle Perception Sensor.

1. Completeness Sensor identifies the paper's four corners in an image. If less than three corners are detected, the image is deemed incomplete.
2. Angle Perception Sensor captures skewness. Given Four points of the image $[x_{0,0}, x_{0,1}, y_{1,0}, y_{1,1}]$, if the angle between line $x_{0,0}, x_{0,1}$ and line $x_{1,0}, x_{1,1}$ is greater than 15 degrees, it is deemed skewness.

A photo that meets any either of the criteria is considered to be of low quality. Overall, there are 386 low-quality images, shown in Table 6

RJUA-MedDQA covers approximately 166 unique diseases and diagnoses for laboratory report, 334 for diagnostic report (non-laboratory report). Of these, 80% are urological-related diseases, and we have listed the top 25 diseases for both report types, shown in Figure 6.

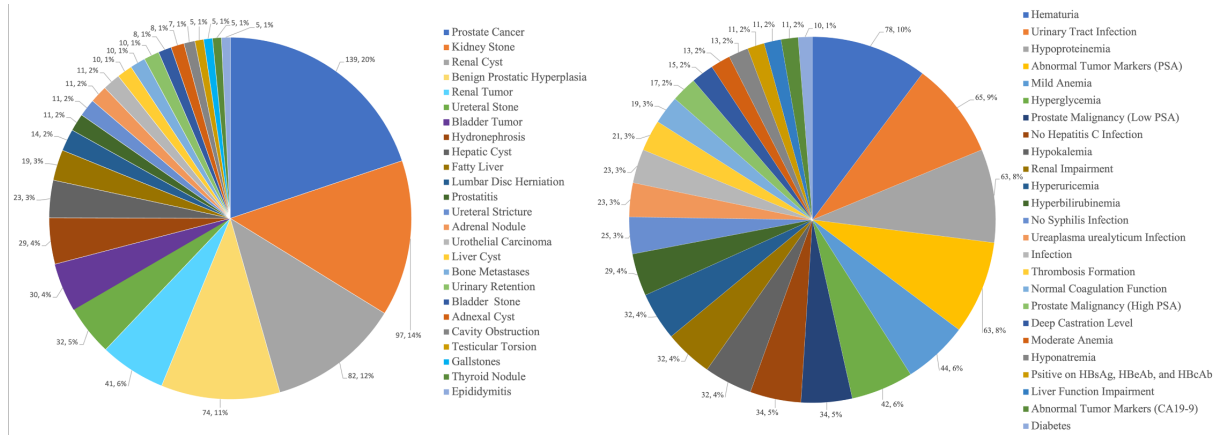
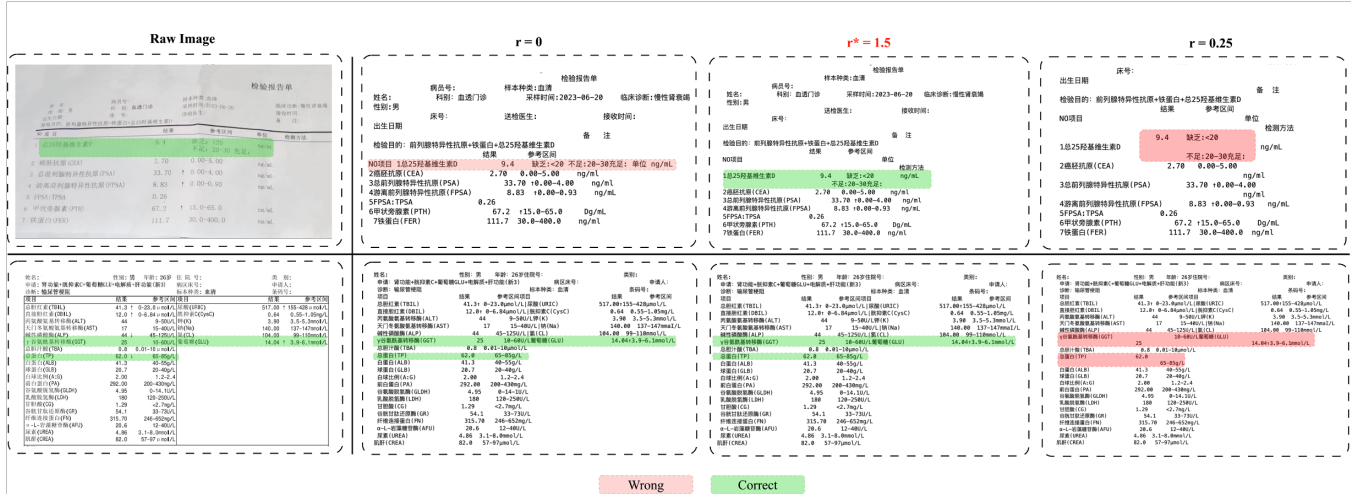


Figure 6: Top 25 Diseases in Laboratory Reports (Left) and Diagnostic Reports (Right)

Figure 7: The Impact of Different r on the output structure of ESRA Structure: An Illustration

B DATA PROCESSING

B.1 Implement Details of ESRA Method

As mentioned in Section 4.1, r^* is a discount coefficient ranging from 0 to 1. By setting this hyper-parameter r^* , the adhesion of text segments between lines can be mitigated, thereby increasing readability. We have tested various settings for r ranging from 0 to 1 (see Figure 7). It can be observed that for electronic raw images (PDF), the impact of r is negligible, whereas for photographs, r results in a more distinct segmentation of each line. We have determined that $r^* = 0.15$ is the optimal value for processing both electronic and photographed images.

l is an expansion coefficient from 0 to 1. By setting the hyper-parameter l , we control the coefficient that determines the number of spaces per line in the overall layout output. $l^* = 0.7$ is optimal.

Table 6: Statistics of Medical Documents in RJUA-MedDQA

Image Type	Quality	# Images	# kv pairs
Photo	High	593	7603
	Low	386	
PDF	High	619	6895
Screenshot	High	402	2351
Overall		2000	16849

B.2 Statistics of RJUA-MedDQA

In this section, we present an overview of the fundamental statistics for the RJUA-MedDQA. This includes the total count of questions and images, the average length of questions, the average length of answers (see Table 7)

We have listed the types and quantities of annotated contexts corresponding to laboratory reports and clinical reports, 178 contexts in total. Notice that laboratory reports do not include contexts

Table 7: Statistics of QAs in RJUA-MedDQA

Task	Answer Type	# Questions	Average Answer Length
Entity	Single	16887	20.8
	Multi	8705	50.2
Table	Single	21784	5.4
	Multi	10892	11.9
TableNR	Single	10892	2.2
	Multi	930	17.3
Reason	MC	1228	12.1
	SA	846	17.2
Overall		72164	17.1

for disease treatments since because it is difficult to extract accurate treatment plans from a single laboratory report. Meanwhile, the lengths of contexts for diagnostic reports are longer than those for laboratory reports. The reason is that the conclusions of laboratory reports are usually related to specific indicators and involve shorter deductive chains, as illustrated in Table 8. In contrast, diagnostic reports include more detailed content based on descriptive observations, such as the dimensions and conditions of the tissues observed, contributing to a variety of therapeutic approaches.

Overall, the clinical reasoning task requires that models have the capability to integrate both the content of images and specific medical information in given contexts in order to derive the correct statement.

Table 8: Statistics of Annotated Contexts. "Exam" denotes Examination

Report Type	Context Type	# Contexts	Average Context Length
Table	Exam-Disease	55	63.1
	Exam-Status	7	86.3
	Disease-Status	1	86
	Disease-Advice	46	71.5
Clinical	Exam	7	61
	Exam-Disease	3	29
	Disease-Exam	16	100.8
	Disease-Status	3	408
	Disease-Treatment	40	310.5
Overall		178	135.1

C EXPERIMENTS

C.1 Impact of Question Difficulty

Based on the data presented in Table 9, it is apparent that for Large Language Models (LLMs), the span of the text containing the answer still influences model performance. The scores for Multi-span are lower than those for Single-span across all tasks, particularly for Table and Table NR task. However, LLMs seem to be less affected, especially for questions within the same row of a table structure, where LLMs (e.g., gpt-4v and qwenvlplus) appear to perform better. Nevertheless, when it comes to reasoning capabilities, there is a significant difference between single indicator anomaly detection

and multi-indicator anomaly detection. The performance of all models on multi-indicator anomaly detection tasks is not ideal. GPT models tend to perform slightly better compared to QWEN models in these tasks.

Table 9: Impact of Question Difficulty on Model Performance. 'S' denotes 'Single'; 'M' denotes 'Multi'

Method	Entity		Table		TableNR	
	S M		S M		S M	
	RougeL	RougeL	Acc	Acc	Acc	Acc
LLaVA-v1.5-7B	0.08	0.07	0.03	0.06	0.37	0.04
mPLUG-Owl2	0.18	0.16	0.01	0.03	0.36	0.20
Qwen-VL-Chat	0.31	0.26	0.14	0.16	0.33	0.22
Qwen-VL-Plus	0.41	0.54	0.53	0.56	0.54	0.19
GPT-4v	0.44	0.47	0.47	0.5	0.50	0.28
ESRA+Qwen	0.84	0.65	0.75	0.72	0.70	0.38
ESRA+GPT-4	0.85	0.76	0.75	0.71	0.64	0.55

C.2 Impact of Image Type

Table 10: Impact of Image Type on Model Performance. "E" denotes "Electronic(PDS/Screenshot)"; "P" denotes "Photo"

Method	Entity		Table		TableNR	
	E P		E P		E P	
	RougeL	RougeL	Acc	Acc	Acc	Acc
LLaVA-v1.5-7B	0.09	0.06	0.04	0.05	0.38	0.32
mPLUG-Owl2	0.20	0.10	0.02	0.02	0.34	0.25
Qwen-VL-Chat	0.31	0.23	0.17	0.09	0.34	0.28
Qwen-VL-Plus	0.47	0.44	0.63	0.36	0.54	0.42
GPT-4v	0.52	0.41	0.52	0.40	0.51	0.41
ESRA+Qwen	0.76	0.81	0.83	0.55	0.72	0.52
ESRA+GPT-4	0.78	0.83	0.82	0.56	0.64	0.54

C.3 Statistics on Hallucination

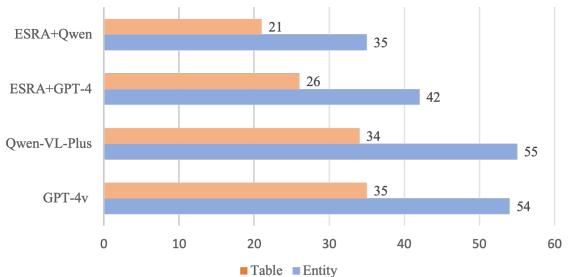
**Figure 8: Statistics on Errors in Hallucination**

Table 11: Impact of Contexts on Model Performance

Method	Multiple Choice									Short Answer								
	Table			Clinical			Table			Clinical								
	Q	C+Q	Δ	Q	C+Q	Δ	Q	C+Q	Δ	Q	C+Q	Δ	Q	C+Q	Δ	Q	C+Q	Δ
Qwen-VL-Plus	0.29	0.3	+0.01	0.28	0.31	+0.03	0.08	0.09	+0.01	0.01	0.01	+0.00						
GPT-4v	0.40	0.48	+0.08	0.38	0.45	+0.07	0.13	0.21	+0.08	0.1	0.19	+0.09						
ESRA+Qwen	0.65	0.72	+0.07	0.45	0.48	+0.03	0.04	0.05	+0.01	0.06	0.01	+0.02						
ESRA+GPT-4	0.70	0.86	+0.16	0.62	0.66	+0.04	0.14	0.22	+0.08	0.22	0.30	+0.08						

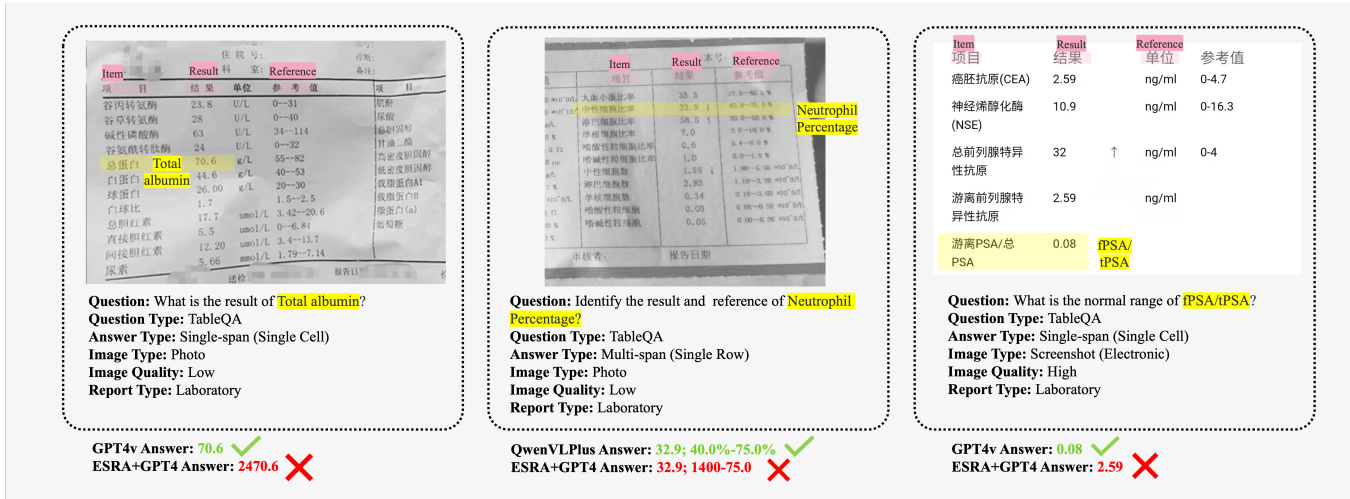


Figure 9: Good cases for low quality image

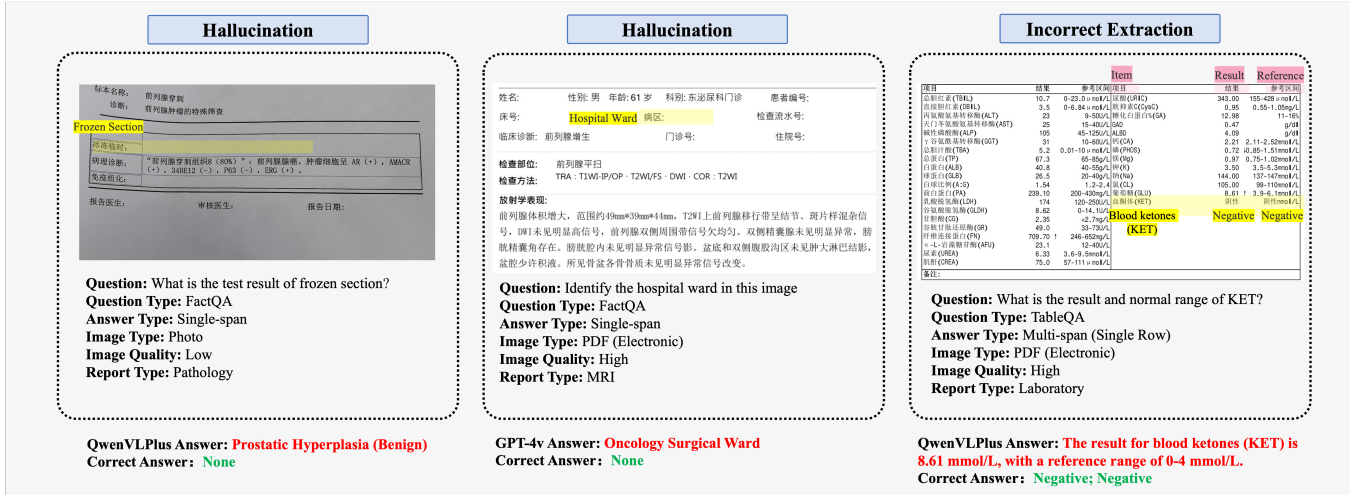


Figure 10: Bad cases for Image Content QA

Faulty Reasoning

Description: 检查方法:上腹部平扫
征象描述:肝脏大小、形态及密度未见明显异常,肝内胆管未见扩张。胆囊区未见明显异常密度高。肝脏、胰腺大小、形态及密度未见明显异常,主胰管未见明显扩张。右侧肾脏长条状高密度影, 约 12mm, 右侧肾盂扩张, 双侧肾上腺、左侧肾脏大小、形态及密度未见明显异常。胃及上腹部肠管未见明显异常, 胃黏膜未见明显肿大淋巴结。胆囊未见明显积液。

Conclusion: 诊断意见:右肾结石, 肾盂扩张积水。

Context: Treatment methods for kidney stones: 1. For small kidney stones less than 1cm that have not caused any symptoms, it is recommended to increase fluid intake and to have regular follow-ups with urinary system ultrasound or CT. Conservative treatment is possible. 2. For kidney stones sized between 1-1.5cm, surgical treatment is recommended, with the preferred method being **ureteroscopic lithotripsy**, followed by percutaneous nephrolithotomy (PCNL) if necessary. Before ureteroscopic lithotripsy, in cases of clear infection, ureteral stricture, larger stone size, a stent may be placed in advance to reduce surgical risk and improve the success rate; the stent is usually kept in place for 1 to 2 weeks. Preoperative use of alpha-receptor blockers can reduce resistance during sheath placement and decrease the risk of requiring ureteral dilation during the procedure. 3. For kidney stones larger than 1.5cm, PCNL is the preferred surgical method.

Question: Based on the context provided and description in the image, choose the correct treatment. Note there is only one correct answer

Options:
A. Conservative treatment with regular follow-ups with urinary system ultrasound or CT;
B. Surgical treatment with preference for ureteroscopic lithotripsy;
C. Surgical treatment with preference for percutaneous nephrolithotomy (PCNL).

Task: Clinical Reasoning
Question Type: AdviceQA
Report Type: CT

QwenVLPlus Answer: C. Surgical treatment with preference for percutaneous nephrolithotomy (PCNL).

Correct Answer: B. Surgical treatment with preference for ureteroscopic lithotripsy

Faulty Reasoning

项目	结果	参考区间	项目
丙肝抗体	0.04	<1.00	
乙肝抗面抗原	4.36 ↑	<1.00	
乙肝表面抗体	34.60 ↑	<10mIU/ml	
乙肝核心抗体	0.008 ↑	>1.000	
乙肝E抗原	0.09	<1.000	
乙肝E抗体	0.86 ↑	>1.000	
HIV Ag/Ab	0.21	<1.000	

Context:
1. Negative syphilis spirochete antibodies suggest no syphilis infection; positive TPPA and negative TRUST indicate syphilis infection.
2. A fasting blood glucose level below 100 mg/dL (5.6 mmol/L) is normal. A level between 100 to 125 mg/dL (5.6 to 6.9 mmol/L) indicates hyperglycemia, suggesting impaired fasting glucose regulation, while a level of 126 mg/dL (7 mmol/L) or higher is indicative of diabetes.
3. **Positive hepatitis B surface antigen, positive hepatitis B core antibody, and positive hepatitis B e antibody** suggest a "minor positivity" status for hepatitis B, also known as "small three positives" for hepatitis B.
4. Negative hepatitis B surface antigen and hepatitis B e antigen suggest no hepatitis B infection; conversely, positives indicate hepatitis B infection.
5. Elevated white blood cell count and CRP levels are typically a response to infection by bacteria, viruses, or other pathogens. The immune system is activated upon infection, leading to an increase in CRP levels.

Question: Based on the context provided and description in the image, choose the correct treatment. Note there is only one correct answer

Options:
A. Syphilis infection; B. Hyperglycemia; C. Hepatitis B "small three positive"
D. No hepatitis B infection E. Infection

Task: Clinical Reasoning
Question Type: DiseaseQA
Report Type: Laboratory

GPT-4v Answer: D. No hepatitis B infection

Correct Answer: C. Hepatitis B "small three positive"

Figure 11: Bad cases for Medical Reasoning MC

Faulty Reasoning

Diagnosis: Bladder Tumor
诊断:膀胱肿瘤

年龄:68岁	病区名称:	床号:		
名族:	性别:	Result:	参考范围:	Reference:
1.10		0.75-1.2		
14.0		11-14.5秒:以INR结果		
凝血酶原时间				
凝血酶原时间	38.4	24-30秒		
凝血酶原时间	16.8	14-21.0秒		
纤维蛋白原定量	3.47	2.0-4.0g/L		
D-二聚体	0.97	≤0.5 μg/g/100ml		
纤维蛋白溶解产物	2.81	(3.0 μg/ml)		
凝血酶原时间	97.00	80%-120%		

Context:
1. Hypoproteinemia, or low protein levels in the blood, is typically confirmed by testing serum albumin and total protein levels. The normal range for total plasma protein concentration is usually 6.4-8.3 g/dL, while the normal range for adult plasma albumin concentration is 3.5-5.5 g/dL. When these values fall below the normal ranges, hypoproteinemia can be considered.
2. **Elevated levels of D-dimer** can indicate the formation of blood clots and have a sensitivity of 95% and a specificity of 40% in the diagnosis of deep vein thrombosis (DVT). A negative result can rule out the possibility of DVT. Studies have shown that cancer can also cause an increase in D-dimer levels in patients, and it can be used as a criterion for staging and prognosis. It is hypothesized that the hypercoagulable state in cancer patients is related to tissue factor-dependent extrinsic pathways and tumor-promoting coagulation functions that are not related to tissue factors. The extrinsic pathway is thought to be activated by the host's monocytes or vascular endothelial cells. An increase in D-dimer levels does not indicate the cause and location of thrombus formation and must be combined with clinical and other test results for analysis.

Question: Based on the context provided and laboratory indicators in the image, provide diagnostic conclusion.

Task: Table Reasoning
Question Type: DiseaseQA
Report Type: Laboratory

QwenVLPlus Answer: Bladder Tumor

Correct Answer: The formation of blood clots

Faulty Reasoning

CT Findings: CT扫描后行轴位MPR重建显示, 肝脏表面光滑, 肝叶比例协调, 肝裂未见明显异常, 肝内小血管清晰可见, 肝内胆管未见明显扩张。脾脏未见明显肿大, 脾门未见明显增粗, 脾内未见明显密度灶, 脾脏大小形态未见明显异常。脾脏形态正常, 大小正常, 密度均匀, 呈明显后缘清晰, 未示明显的大淋巴结, 双肾形态正常, 左右肾小盏圆形稍高密度影, 双肾乳头未见明显增粗, 双肾门未见明显肿大, 左肾未见明显异常, 右肾未见明显异常, 双肾密度影, 未见异常强化灶。

CT Impression: CT印象:
1. 左肾稍高密度灶, 考虑高密度小囊肿, 建议随访复查;
2. 肝脏多发小囊肿, 随诊。

Context:
Treatment of kidney cysts depends on the nature of the cyst (benign or malignant), size, whether it causes symptoms, and whether it affects kidney function. Most kidney cysts are benign and do not always require treatment.
1. **Conservative Treatment for Kidney Cysts:** For small cysts (**less than 3.5cm**) that are asymptomatic and do not affect kidney function, a watchful waiting approach with regular monitoring is typically adopted. This may include regular ultrasound or CT scans to monitor the cyst's size and properties.
2. **Aspiration and Sclerotherapy for Kidney Cysts:** Kidney cysts measuring 4-8cm may be considered for aspiration under ultrasound or CT guidance, where a needle is used to puncture the cyst and withdraw the fluid. Sclerotherapy: After aspirating the cyst fluid, a sclerosing agent may be injected to reduce the likelihood of cyst recurrence.
3. **Decortication and Decompression Surgery for Kidney Cysts:** For cysts larger than 8cm or those compressing the renal pelvis, surgical removal of the cyst is recommended, using laparoscopic decortication and decompression surgery.
4. **Treatment for Kidney Cysts (Bosniak Category III or higher):** If the cyst is suspected or confirmed to be malignant, partial nephrectomy is recommended for treatment. If the kidney cannot be preserved, radical nephrectomy is indicated.

Question: Based on the context provided, finds and impression in the image, provide diagnostic treatment

Task: Clinical Reasoning
Question Type: AdviceQA
Report Type: CT

GPT-4v Answer: Renal cyst

Correct Answer: Conservative treatment with regular ultrasound or CT scans to monitor the size and characteristics of the cyst.

Figure 12: Bad cases for Medical Reasoning SA

Faulty Reasoning

检查部位: 盆腔平扫增强
检查方法: TRA: T1WI/JP - T2WI/FS - DWI - COR - T2WI, 增强 (磁共振对比剂15ml, 静脉注射, 浓度#1.5ml/s)TRA: LAVA/mDixon/eThrive二期扫描
放射学表现: **Radiological Findings**

“前列腺癌治疗后改变”，膀胱导尿管置留中。前列腺体积增大，向上突向膀胱底，T1WI上见小斑片高信号影。左侧周围带中部截石位3-4点见斑片状DWI高信号，ADC值减低，直径约16mm。T2WI上前列腺移行带混杂信号，见多发小斑片DWI稍高信号，ADC值略减低，注入对比剂后见不均强化。左侧精索腺信号不均匀伴局部DWI稍高信号，膀胱精囊角存在。膀胱前壁稍毛糙，前缘见囊袋样影。盆底、双侧腹股沟区及膀胱旁多发淋巴结影，盆腔内未见明显积液。所见骨骼部分组成骨骨质信号不均。

Radiological Diagnosis:

放射学诊断: **Prostate cancer with invasion of the left seminal vesicle gland.**

- “前列腺癌治疗后改变”，前列腺癌并侵犯左侧精囊腺：盆底、双侧腹股沟区及膀胱旁多发淋巴结。请结合病史及PSA等复查。**Pelvic floor, inguinal regions bilaterally, and multiple lymph nodes around the iliac vessels.**
- 前列腺少许出血。
- 膀胱导尿管置留中。膀胱前缘憩室。
- 骨盆部分组成骨骨质信号不均。请结合骨扫描检查。

The bone signal of the pelvic bones is heterogeneous. Please refer to bone scan examination.

Question: Based on the context provided, description and conclusion in the image, identify the TNM staging of prostate cancer.

Task: Clinical Reasoning

Question Type: StatusQA

Report Type: MRI

Context:
TNM staging is a system used to describe the extent of cancer spread in the body. It is commonly used for many types of cancer, including prostate cancer, to assess the disease progression and to determine the most appropriate treatment approach. The TNM classification is based on three criteria:

- ❖ **T (Tumor):** Describes the size of the original (primary) tumor and whether it has invaded nearby tissue. In the context of prostate cancer, the T categories range from T1 to T4,
 - T0: No evidence of primary tumor.
 - T1: Clinically inapparent tumor not palpable nor visible by imaging.
 - T1a: Incidental tumor present in 5% or less of the resected tissue.
 - T1b: Incidental tumor present in more than 5% of the resected tissue.
 - T1c: Tumor not palpable, identified by needle biopsy (e.g., due to elevated PSA).
 - T2: Tumor palpable and confined within the prostate.
 - T2a: Tumor involves one-half of one lobe or less ($\leq 1/2$).
 - T2b: Tumor involves more than one-half of one lobe, but not both lobes.
 - T2c: Tumor involves both lobes.
 - T3: Tumor extends through the prostate capsule.
 - T3a: Tumor invades through the capsule (one side or both sides).
 - T3b: Tumor invades the seminal vesicles.
 - T4: Tumor is fixed or invades adjacent structures other than the seminal vesicles, such as the bladder neck, external sphincter of the urethra, rectum, levator muscles, and/or pelvic wall.
- ❖ **N (Nodes):** Indicates whether the cancer has spread to nearby lymph nodes and if so, the extent of the spread.
 - Nx: Regional lymph nodes cannot be assessed.
 - N0: No regional lymph node metastasis.
 - **N1:** Regional lymph node metastasis.
- ❖ **M (Metastasis):** Indicates whether the cancer has spread (metastasized) to other distant parts of the body
 - **Mx:** Metastasis cannot be assessed.
 - M0: No distant metastasis.
 - M1: Distant metastasis.
 - M1a: Metastasis to non-regional lymph nodes.
 - M1b: Bone metastasis.
 - M1c: Metastasis to other organs, with or without bone metastasis.

GPT-4vs Answer: **T2aN0M0**
Correct Answer: **T3bN1Mx**

Figure 13: Bad cases for Medical Reasoning SA

Table 12: Examples of Annotated Contexts

Type	Title	Type	Description
Lab	Mild Anemia	Exam-Disease	A hemoglobin level of 90g/L to 120g/L indicates the presence of mild anemia; A hemoglobin level of 60g/L to 90g/L indicates the presence of moderate anemia.
Lab	Malignant Prostate Tumor (Low PSA)	Exam-Disease	In patients with malignant prostate tumors, high levels of PSA are associated with a higher tumor burden; low levels of PSA indicate a better treatment response and a lower tumor burden.
Lab	Poor Prognosis for Testicular Tumors	Disease-Status	Elevated LDH levels suggest a poor prognosis for patients with testicular tumors; pre-chemotherapy LDH levels can be used as a prognostic factor for overall survival (OS) in the intermediate-risk group of non-seminomas. In seminomas, lactate dehydrogenase (LDH) has been proven to be an additional adverse prognostic factor.
Lab	Thrombosis Formation (High Coagulation Risk)	Disease-Advice	Thrombosis formation can be treated with low-molecular-weight heparin or further monitored using thromboelastography or TAT/PIC levels.
Clinical	Renal Cysts Treatment	Disease-Treatment	<p>Treatment of kidney cysts depends on the nature of the cyst (benign or malignant), size, whether it causes symptoms, and whether it affects kidney function. Most kidney cysts are benign and do not always require treatment.</p> <ol style="list-style-type: none"> 1. Conservative Treatment: For small cysts (less than 3.5cm) that are asymptomatic and do not affect kidney function, a watchful waiting approach with regular monitoring is typically adopted. This may include regular ultrasound or CT to monitor the cyst's size and properties. 2. Aspiration and Sclerotherapy: Kidney cysts measuring 4-8cm are considered for aspiration under ultrasound or CT guidance, where a needle is used to puncture the cyst and withdraw the fluid. Sclerotherapy: After aspirating the cyst fluid, a sclerosing agent may be injected to reduce the likelihood of cyst recurrence. 3. Decortication and Decompression Surgery: For cysts larger than 8cm or those compressing the renal pelvis, surgical removal of the cyst is recommended, using laparoscopic decortication and decompression surgery. 4. Treatment for Kidney Cysts (Bosniak Category III or higher): If the cyst is suspected or confirmed to be malignant, partial nephrectomy is recommended for treatment. If the kidney cannot be preserved, radical nephrectomy is indicated.

Table 13: Examples of Medical Knowledge-based Synonym-aware Schema

Topic	Key Entity	Synonyms
Basic Information	Name	Patient
	Age	DateofBirth
	Date	Examination Date, Test Date, Report Date, Writing Date, Date Received, Audit Date, Submission Time, Specimen Acceptance Time, Report, Audit
	pre-test Diagnosis	Clinical Diagnosis
Laboratory	Item	Examination Item, Test Item, Indicator, Laboratory Indicator
	Result	Examination Result, Laboratory Result, Test Result
	Range	Referene Range, Normal Range, Standard Range, Normal Interval
CT	Description	CT Appearance,
	Conclusion	CT Diagnosis, CT Impression
Endoscopic	Description	Cystoscopy Description, Endoscopic Description
Ultrasound	Description	Ultrasound Description, Ultrasound Findings, Ultrasound Contrast, TRUS
Pathology	Description	Frozen Section, Immunohistochemistry, Macroscopic Examination, Microscopic Findings
	Conclusion	Pathological Diagnosis, Supplementary Pathological Diagnosis, Comprehensive Evaluation
General	Description	Radiological Appearance, Imaging Appearance, Observation records, Examination findings, Inspection findings, Film indication, Impression note
	Conclusion	Radiological Diagnosis, Imaging Diagnosis, Imaging Conclusion, Clinical diagnosis, Examination diagnosis, Imaging findings, Conclusions and Recommendations, Diagnosis, Diagnostic Opinion, Impression